FARADAY

FTIR study of defects produced in ZrO_2 samples by thermal treatment

Residual species into cavities and surface defects

Marco Daturi,[a]† Claude Binet,[a] Serafin Bernal,[b] José A. Pérez Omil[b] and Jean Claude Lavalley[a]*

[a] *Laboratoire de Catalyse et Spectrochimie, UMR 6506, ISMRA, 6, Bd. du Maréchal Juin, 14050 Caen Cedex, France.*

[b] *Departamento de Química Inorgánica, Facultad de Ciencias, Universidad de Cádiz, Poligono Rio San Pedro, 11510 Puerto Real/Cádiz, Spain*

The effect of two different thermal/chemical pretreatments on a high surface area zirconia sample has been studied using FTIR spectroscopy. As revealed by high resolution electron microscopy (HREM), the sample exhibits a significant concentration of small pores and cavities with size ranging from 1 to 2 nm. When pretreatment 1 was applied, (step-by-step heating under O_2 followed by evacuation at increasing temperatures up to 873 K), the oxide appeared clean, and free from impurities detectable by IR spectroscopy. Likewise, no O_2^- species resulting from further O_2 chemisorption at 298 K were observed. In contrast, the IR spectrum for the oxide exposed to pretreatment 2 (heating under O_2 at 873 K, followed by fast evacuation at 873 K), shows a number of features that can be interpreted as due to oxalate-like species, as well as adsorbed CO. Additionally, superoxide species could be identified upon O_2 chemisorption at room temperature. Further reoxidation treatment at 673 K induces the disappearance of CO features and the transformation of the oxalate-like species. The initial spectrum can be recovered by subsequent evacuation at 873 K, thus indicating the reversible nature of the chemical processes involved. In accordance with the HREM images, we propose that a redox interconversion reaction of chemisorbed species trapped in the oxide cavities is responsible for what we observe on the zirconia sample exposed to pretreatment 2.

ZrO_2 is an important material in the field of heterogeneous catalysis.[1,2] It is well known as a stable oxide which tends to loose surface oxygen only after thermal treatment under high vacuum, above 973 K.

In the literature there are many examples of O_2^- species formation over the surface of several oxides, such as MgO, CaO, SrO, Co_2O_3, Cr_2O_3 and ZnO,[3–9] when O_2 is adsorbed after a reducing treatment under hydrogen. Other oxides, like Fe_2O_3 or CeO_2, show the presence of superoxides on their surfaces after thermal treatment under dynamic vacuum, severe enough to create anionic vacancies on the oxide surfaces.[10–16] All the proposed mechanisms concerning superoxide formation imply the presence of surface defects (anionic vacancies or doping elements), where O_2^- species are formed by O_2 coordination with cations of high electron donor properties.[3,5,12,13,16] Thus, O_2^- species formation is used here to prove the existence of such surface defects.

Up till now, evidence of superoxide species on zirconia surface by FTIR spectroscopy have been reported only by Jacob *et al.*,[17] after reducing treatment in H_2 atmosphere, in order to obtain a significant concentration of surface radical H^0 defect sites. In our work only calcination and vacuum treatment at moderate temperature were performed, with the aim of ultimately purifying the sample, discarding the presence of H^0 defect sites. In the two experimental conditions used here for sample pretreatment, more or less good equilibration of the ZrO_2 sample with oxygen during the calcination process greatly influences the formation of structural defects.

The aim of the present study is to investigate surface defects according to sample pretreatment. Additionally, the IR studies allowed us to detect cavities through the remaining impurities that depend on the pretreatment, and these studies are confirmed by high resolution electron microscopy.

Experimental

ZrO_2 oxide powder was specifically prepared from its nitrate precursor by Rhône-Poulenc for this study. The specific surface area of the powder was 89 $m^2\ g^{-1}$ as measured by the low temperature adsorption isotherm of N_2, on an ASAP 200 Micromeritics instrument. The adsorption isotherm was of type II, while only a very narrow hysteresis loop of H1 type was observed (IUPAC codification). These results indicate a solid constituted by a rigid packing of particles having uniform diameters with intertwining macroporosity (pore diameter >50 nm). The *t*-plot analysis of the isotherm shows that the microporosity is very low and no significant value was obtained above the limit of detection using N_2 as adsorbant (pore diameter >2 nm). From X-ray diffraction measurements (XRD), *via* the Scherrer method, the diameter of the crystallites was found to be *ca.* 7–10 nm.

High resolution electron microscopy (HREM) images were recorded on a JEOL-2000-EX microscope with 0.21 nm point resolution. The instrument was equipped with a top-entry specimen holder and an ion pump. The experimental micrographs were digitised on a CCD camera, COHU-4910. Digital processing was performed using the SEMPER-6+ software. For IR studies the powders were pressed into self supported wafers of about 10 mg cm^{-2} and activated *in situ* in a quartz cell, placed into the IR beam.

Two types of treatments have been applied: (i) a step-by-step cleaning treatment, heating under 1.3×10^4 Pa of O_2 for 1 h followed by evacuation for 1 h under dynamic vacuum ($P \approx 10^{-4}$ Pa) up to 873 K, with steps at 373, 473, 623 and

† On leave from the Istituto di Chimica, Facoltà di Ingegneria, Università di Genova, P.le J.F. Kennedy, 16129 Genova, Italy.

773 K; (ii) a quick treatment, heating under 1.3×10^4 Pa of O_2 for 1 h followed by evacuation for 1 h under dynamic vacuum ($P \approx 10^{-4}$ Pa) at 873 K. IR spectra were recorded at room temperature (rt) with a Nicolet Magna 550 FTIR spectrometer (resolution 4 cm^{-1}) after quenching the samples at room temperature. The spectra have been treated using the Nicolet OMNIC software.

Results and Discussion

HREM characterisation study of the zirconia sample

Fig. 1 accounts for a representative HREM micrograph of the oxide sample investigated here. By digital processing of the image, the digital diffraction pattern (DDP) (inset in Fig. 1) could be obtained. This DDP is consistent with monoclinic zirconia crystals in [011] orientation. Also, in accordance with the HREM image in Fig. 1, the sample shows very small regions (1–2 nm) where the average brightness of the HREM image is higher than that of the surroundings. These bright areas, which are marked with arrows in Fig. 1, can be interpreted as due to regions with lower density of dispersing material, *i.e.* to the presence of pores and cavities in the oxide sample. This textural feature is consistent with the high surface area, and therefore, low calcination temperature, applied during sample preparation. Likewise, as will be discussed below, the presence in our zirconia sample of such a porosity will provide one of the clues for understanding the differences observed in the FTIR spectra of the oxide as a function of the applied pretreatment.

Occluded species

If we submit the sample to a quick treatment, such as 1 h in O_2 at 873 K followed by 1 h under dynamic vacuum at the same temperature, we do not obtain the spectrum of a clean sample, but the features of residual carbonate/carboxylate-like compounds at 1544, 1499, 1358, 1334, 1310 (shoulder) and 1255 cm^{-1} [Fig. 2A, spectrum (a)]. Upon reoxidation with O_2 (13 kPa, 673 K), the intensity of the bands near 1544, 1360 and 1310 cm^{-1} grows at the expense of those located at 1499, 1334 and 1255 cm^{-1} that almost completely vanish [Fig. 2A, spectrum (b)]. Thus, the former triplet of the band is assigned to an S species, while the latter to an S′ one. Further evacuation at 873 K [Fig. 2A, spectrum (c)] gives spectrum (a) again. The appearance of species S′ upon evacuation and their disappearance upon reoxidation is a reversible process. We then conclude that S′ species are transformed into S species.

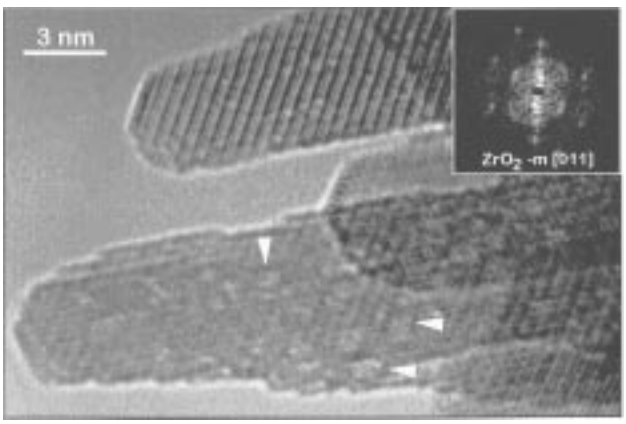

Fig. 1 HREM image corresponding to the ZrO_2 sample. The DDP inset can be interpreted as due to monoclinic zirconia in [011] orientation. The small bright areas, like those marked with arrows, are associated to pores and cavities in the sample.

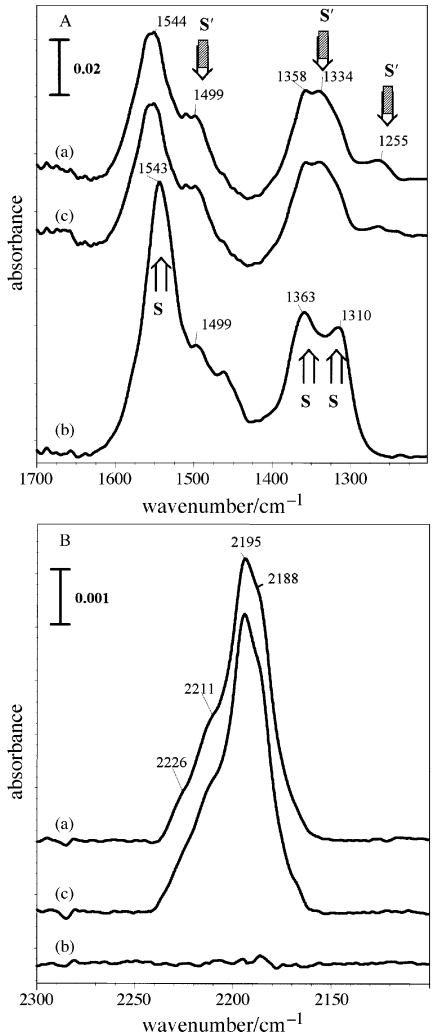

Fig. 2 A, FTIR spectra in the carbonate–carboxylate vibrational range after evacuation at 873 K (quick treatment) (a), reoxidation with O_2 at 673 K (b) and subsequent evacuation at 873 K (c). B, FTIR spectra in the carbon monoxide vibrational range; (a), (b) and (c): the same as for A.

Bands characterising S′ species (1499, 1334, 1255 cm^{-1}) are analogous to those due to S species (1544, 1360, 1310 cm^{-1}) but they are shifted to lower frequencies. This infers that S and S′ species are structurally identical, but differing from the properties of their anchoring site, possibly from effects induced by some coadsorbed species (see below).

Considering now the ν(CO) stretching mode spectral range, similar conclusions, reinforcing the above ones, are reached: (i) after the step-by-step cleaning treatment of ZrO_2, no band appeared in the ν(CO) spectral range. (ii) In contrast, after the quick cleaning thermal treatment and after cooling to rt under vacuum, ν(CO) bands are seen at 2195 and 2188 cm^{-1}, with shoulders at 2226 and 2211 cm^{-1} [Fig. 2B, spectrum (a)]. The presence of such bands under vacuum at rt clearly indicates that they are not due to some adsorbed CO species on the external surface, but to occluded ones, which is confirmed by the absence of any isotopic exchange after heating at 873 K in the presence of ^{13}CO. Then, S, S′ and CO species may be present in internal cavities. Moreover, sample reoxidation at 673 K [Fig. 2B, spectrum (b)] leads to complete disappearance of the ν(CO) bands which are reversibly restored upon evacuation at 873 K [Fig. 2B, spectrum (c)]. The disappearance of CO occluded species upon reoxidation is unaccompanied by the appearance of species other than S. Then CO, S and S′ species in cavities are closely related; some of the S (or S′) species are reversibly decomposed into CO ones upon evacuation at 873 K.

For comparison, CO was physically adsorbed on the zirconia external surface under 1.3 kPa of CO at rt [Fig. 3(a)]. Two bands are observed at 2196 and 2187 cm^{-1} *i.e.* at the same frequencies, and with nearly the same relative intensities as the main bands above assigned to CO into cavities (Fig. 2B). As expected for adsorbed CO species on the external surface, these species desorb upon outgassing at rt [Fig. 3(b)]. In the literature[18,19] ν(CO) bands at 2196 and 2187 cm^{-1} were assigned to CO species adsorbed on two distinct coordinatively unsaturated surface Zr^{4+} ions. It was suggested that the band with the highest wavenumber (2196 cm^{-1}) was due to CO adsorbed on surface crystal defects such as edges, corners, *etc.*, while the other (2187 cm^{-1}) being assigned to CO adsorption on less coordinatively unsaturated Zr^{4+} ions located on surface terraces.[19] So, (i) the main ν(CO) bands observed in this work (Fig. 2B) are assigned to occluded CO adsorbed on coordinatively unsaturated and unreduced Zr^{4+} ions, but (ii) we discard the assignment of these bands to CO adsorbed on Zr^{4+} ions located either on surface defects or on Zr^{4+} on terraces. Indeed, the same relative importance of these bands for CO adsorbed on the internal surface of cavities (Fig. 2B) and for CO adsorbed on the external surface [Fig. 3(a)] shows that the distinction between the corresponding two types of Zr^{4+} sites cannot be related to the relative importance of faces and edges (or corners), which is *a priori* very different for the internal surface of small cavities and for the extended external surface. The presence of two types of Zr^{4+} surface sites has to be related only to local structures of the surface, without specific correlation with faces and edges.

The ν(CO) shoulders at 2226 and 2211 cm^{-1} [Fig. 2B, spectrum (a)] would be assignable to very intrinsically acidic Zr^{4+} sites located into the cavities, but such high frequency bands had never been observed for CO adsorbed on clean ZrO_2 surfaces. We preferred to assign them to an induced effect of coadsorbed S (or S′) species shifting the pair of bands from 2195, 2188 cm^{-1} to 2226, 2211 cm^{-1}. In the literature such ν(CO) shifts toward higher frequencies have been observed for surface sulfated[20] or carbonated[21] zirconia and assigned to SO_4^{2-} and CO_3^{2-} inductive effects at the CO adsorption site. If cavities are not large, coadsorbed species would be in close vicinity, and a high induced effect is expected. In this interpretation, S′ species may be S species but coadsorbed with CO, the coadsorption increasing at the same time as the acidity at the CO adsorption sites and the basicity at the S′ adsorption ones. Thus, a downward shift for the observed S frequencies takes place.

For CO trapped in zeolitic supercages, whose diameter would be evaluated to be about 1.4 nm, bands at 2207, 2192, 2178 and 2165 cm^{-1} were ascribed to $(CO)_n$ molecular clusters stabilised under cation fields.[22] The bands here observed at 2156 and 2187 cm^{-1} may not be assigned to such clusters because they are observed both for CO adsorbed at the external surface and inside the cavity. Moreover, considering the weak dipole moment of CO, such polymeric $(CO)_n$ species would be observed at very low temperatures, with wavenumbers not far from that of a liquid-like state (*i.e.* near 2140 cm^{-1}); we then discarded assignment of the bands we observed here at 2226, 2211 cm^{-1} to such hypothetical clusters.

We have also investigated the possible reducing effect of H_2 on our sample when processing it at 873 K. This temperature is in fact sufficient to obtain a large number of cations in a reduced state of oxidation in many oxides. After this treatment under hydrogen, the spectrum of occluded S, S′ and CO species is left unchanged (see Fig. 4 compared with Fig. 2). This shows that up to this temperature, H_2 has no reducing effect, at least in the bulk, viewing as probes the cavities hollowed in it.

Surface defects

The question is now, how do the experimental conditions influence the nature of the residual species located in internal cavities? As shown above, the nature of these species depends reversibly either upon sample evacuation at 873 K or upon its oxidation at 673 K. This implies a redox process for the change in the chemical nature of the occluded species. Furthermore, the adsorption of the CO spectroscopic probe (Fig.

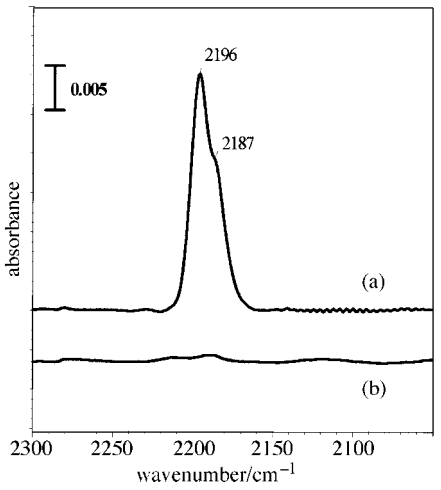

Fig. 3 FTIR spectrum of the sample after adsorption of 1.3 kPa of CO at rt (a) and after evacuation at rt (b)

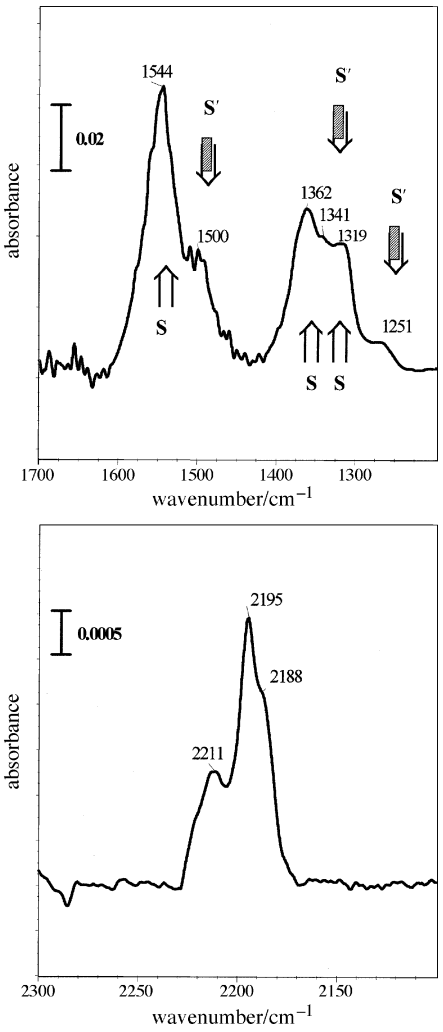

Fig. 4 FTIR spectrum of the sample H_2-treated at 673 K, after evacuation at 673 K

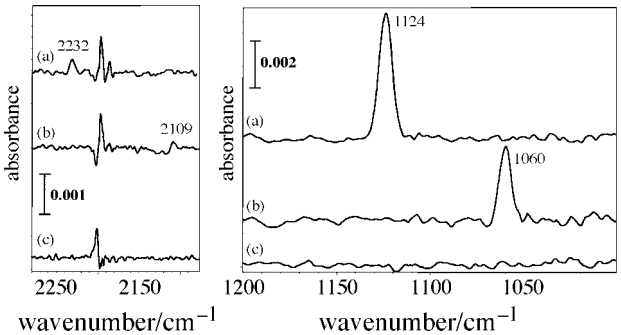

Fig. 5 FTIR spectra of adsorbed dioxygen on the sample 10 min after introduction of 13 kPa of $^{16}O_2$ at rt (a), 1.3 kPa of $^{18}O_2$ at rt (b) and 13 kPa of $^{16}O_2$ at 673 K and cooled down to rt (c). A, spectral range of the first overtone; B, spectral range of the O—O bond vibration. These spectra are differences between those obtained after and before the introduction of O_2.

3) only indicates the presence of Zr^{4+} ions, expectedly discarding any important reduction of ZrO_2 upon evacuation at 873 K, but retaining the possibility of the formation of some minor reduced surface defects. To test this last hypothesis, O_2 was adsorbed at rt on the sample quickly evacuated at 873 K. Superoxide O_2^- species were thus formed and characterised by their ν(O—O) stretching mode at 1124 cm^{-1} and its first overtone at 2232 cm^{-1} [Fig. 5(a)]. The 1124 cm^{-1} value is very near the 1118 cm^{-1} one for O_2^- species on H_2–O_2 coadsorbed on ZrO_2[17] or coincides, as well as its overtone, with the values (1126 and 2237 cm^{-1}) observed for O_2^- adsorbed on evacuated ceria.[11,12] By adsorbing $^{18}O_2$ instead of $^{16}O_2$ [Fig. 5(b)] the 1124 → 1060 cm^{-1} and 2232 → 2109 cm^{-1} isotopic shifts confirm the attribution of these bands to a ν(O—O) vibration. As surface O_2^- species are produced at rt, the spectra of occluded species is left unchanged. Only minor features appear as differences in the ν(CO) spectral range at around 2200 cm^{-1} in Fig. 5, but they are not significant in these subtraction spectra, taking into account the absorbance scale. In contrast [Fig. 5(c)], O_2^- species are not observed upon heating under oxygen at 673 K. Then O_2 adsorption at rt shows the presence of some reduced surface defects without reoxidation or perturbation of occluded impurities. While heating under O_2 at 673 K destroys the surface defects, the oxidation is then transmitted to the cavities (see above).

It was proposed that O_2^- species adsorbed on zirconia by the H_2–O_2 coadsorption were produced *via* the interaction of hydride H^- surface species with O_2.[17] In our experimental conditions, which exclude any H_2 treatment, such a proposal has to be discarded. The formation of O_2^- species is not observed for our sample for which step-by-step cleaning treatment has been applied, but only when the sample is quickly pretreated. This suggests that the fast decomposition of surface impurities upon thermal evacuation leads to surface reduced defects. The nature of these reduced defects may either be Zr^{3+} ions associated with O vacancies or colour surface centres constituted by O vacancies containing one electron (F_s^+ centre) or two electrons (F_s centre). This shows that, during the step-by-step slow cleaning treatment, the surface is allowed to be re-equilibrated and no reduced surface defects are observed.

Redox process transmission from the external surface to internal cavities

The nature of S species which reversibly transform into CO upon reduction may be assessed from the IR bands at 1544, 1360 and 1310 cm^{-1}. They are located in the spectral range where two $\nu(CO_3)$ bands are generally found for adsorbed CO_3^{2-} carbonate species. The presence of a third band in this spectral range suggests a little more extended structure; we then assume that the S species is a head-to-tail oxalate $C_2O_4^{2-}$ species. Such a species was supposed to occur, for example, as impurities on chlorinated ceria samples with bands at 1487, 1372 and 1340 cm^{-1};[23] such a structure for S species fits well in Scheme 1, elaborated here to explain the equilibration of the local surface redox state with the cavity. In Scheme 1 we suppose that the treatment under vacuum at high temperature produces local reduction of the surface, which recalls neighbour oxygens from the bulk and partially changes the coordination inside the cavities, acting as a reducing element. The reoxidation of the surface produces a relaxation of the network and reconstitution of the previous species inside the cavities. This process involves a mass transport of oxygen between cavities and the surface, which is assumed to be a propagation of the defects at high temperatures, by a hopping O displacement through neutral O vacancies (see Scheme 1 and the mechanism proposed below). Note that occlusions are not necessarily deeply embedded into the bulk. The overall redox process is limited by the amount of available external surface defects explaining then that oxalate species into cavities may be found either unreduced (S species), reduced into CO species or coexisting with CO (S′ species). In Scheme 1, two Zr^{4+} sites for occluded CO adsorp-

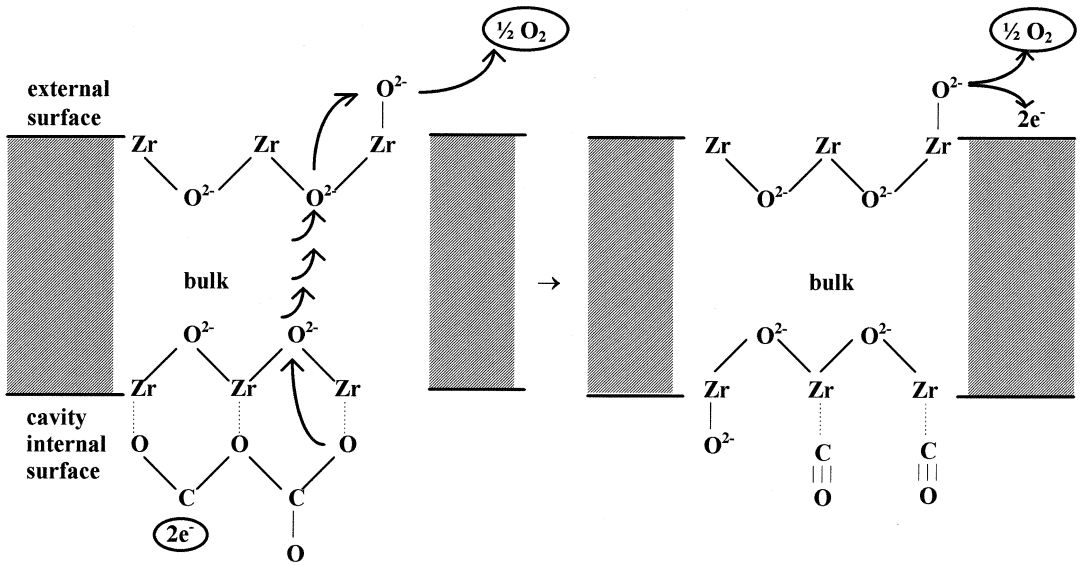

Scheme 1 Tentative interpretation of the mechanism of reduction and reoxidation on the external surface of the sample and on the internal surface of the cavities: occluded CO reversible formation

tion are considered. One is in the proximity of a capping basic O^{2-} species describing a Zr^{4+} site less acidic than the other one and justifying the observation of two ν(CO) bands (2188 and 2195 cm^{-1}). Very similar Zr^{4+} sites are considered for the external surface in Scheme 1, to take into account the similarity of CO adsorption on the external surface and into the cavities.

Note that the exact nature of the capping O^{2-} species in Scheme 1 is somewhat unknown; the representation here used is only indicative of its easy removal upon thermal treatment.

The mechanism of the defects–oxygen interaction can be written in the following way:

$$O_{surf}{}^{2-} \rightarrow \tfrac{1}{2}O_2 + V_{O,\,surf}$$

$$V_{O,\,surf} + O_{bulk(n)}{}^{2-} \rightarrow O_{surf}{}^{2-} + V_{O,\,bulk} + O_{bulk(n-1)}{}^{2-}$$

$$V_{O,\,bulk} + C_2O_4{}^{2-} \rightarrow 2CO_{cavity} + O_{bulk}{}^{2-} + O_{cavity}{}^{2-}$$

which leads to the general equation for the oxalate reversible decomposition

$$C_2O_{4\ cavity}{}^{2-} = 2CO_{cavity} + O_{cavity}{}^{2-} + \tfrac{1}{2}O_2$$

In the mechanism above, V_O indicates a neutral O-vacancy (*i.e.* a vacancy having two electrons).

Origin of the textural defects

As the ZrO_2 sample was prepared from zirconium nitrate, the observed oxalate impurities are not due to the precursor. However, unavoidable atmospheric CO_2 adsorption on ZrO_2 leads to the formation of carbonate species, possibly during the precalcination process at low temperature. Then, small nanopores (1–2 nm) as evidenced by the HREM study, but too small to be detected through adsorption–desorption N_2 isotherms (see Experimental), may be anchoring sites for carbonate species. The carbonates so formed are thought to be more thermally stable than carbonate species on the external surface, that are entirely destroyed during thermal treatment. It is plausible that some pores close during either the quick or the step-by-step slow thermal treatments. The resulting cavities would be free from impurities in the case of the slow step-by-step thermal treatment, allowing carbonate decomposition products to escape before pore closure. In contrast, oxalate-like species resulting from carbonate reduction are thought to be trapped in the pore closure process during the quick thermal treatment.

Conclusion

Carbonate impurities are assumed to be present in small pores (*ca.* 2 nm) in the untreated ZrO_2 sample. The cleaning thermal treatment up to 873 K is expected to give rise to the closure of the pores. If the temperature increase during thermal treatment is slow (step-by-step), impurities escape before the pore closure, and a very clean ZrO_2 sample is effectively obtained. In the opposite treatment, (quick treatment followed by a rapid quench at rt), impurities are left in the bulk of the sample in the form of occluded species. These species, assumed to be head-to-tail oxalates, located inside cavities into the bulk are useful for characterising the bulk using surface techniques. When the sample is locally reduced on the surface by evacuation, electron transfer into the cavities occurs, which gives rise to the reduction of the postulated oxalate species into CO. This transformation is totally reverted after reoxidation at 673 K. Impurities trapped in cavities act like bulk pinning centres for surface defects.

Very similar ν(CO) bands at 2195 and 2188 cm^{-1} were observed for CO adsorbed either into cavities or onto the external surface, unexpectedly with approximately the same relative importance. This infers that, as suggested in the literature, a one-to-one correspondence of one of the bands with surface terraces (2188 cm^{-1}) and the other band (2195 cm^{-1}) with edges is questionable. Induced effects on frequencies were observed for CO and oxalate species coadsorbed into cavities.

The authors are grateful to the European Commission for the financial support received from the TMR Program [Contract FMRX-CT-96-0060(DG12-BIUO)].

References

1 K. Tanabe and T. Yamaguchi, *Catal. Today*, 1994, **20**, 185.
2 T. Yamaguchi, *Catal. Today*, 1994, **20**, 199.
3 S. Coluccia, F. Boccuzzi, G. Ghiotti and C. Morterra, *J. Chem. Soc., Faraday Trans.*, 1982, **78**, 2111.
4 A. J. Tench, T. Lawson and J. F. J. Kibblewhite, *Trans. Faraday Soc.*, 1972, **68**, 1169.
5 T. Ito, M. Yoshioka and T. Tokuda, *J. Chem. Soc., Faraday Trans.*, 1983, **79**, 2277.
6 E. Giamello, E. Garrone, P. Ugliengo, M. Che and A. J. Tench, *J. Chem. Soc., Faraday Trans.*, 1989, **85**, 3987.
7 E. Giamello, Z. Sojka, M. Che and A. Zecchina, *J. Phys. Chem.*, 1986, **90**, 6084.
8 A. A. Davydov, *J. Chem. Soc., Faraday Trans.*, 1991, **87**, 913.
9 B. K. Na, A. B. Walters and M. A. Vannice, *J. Catal.*, 1993, **140**, 585.
10 F. Al-Mashta, N. Sheppard, V. Lorenzelli and G. Busca, *J. Chem. Soc., Faraday Trans.*, 1982, **78**, 979.
11 C. Li, K. Domen, K. Maruya and T. Onishi, *J. Chem. Soc., Chem. Commun.*, 1988, 1541.
12 C. Li, K. Domen, K. Maruya and T. Onishi, *J. Am. Chem. Soc.*, 1989, **111**, 7683.
13 J. Soria, A. Martínez-Arias and J. C. Conesa, *J. Chem. Soc., Faraday Trans.*, 1995, **91**, 1669.
14 X. Zhang and K. J. Klabunde, *Inorg. Chem.*, 1992, **31**, 1706.
15 C. Li, Q. Xin and X. Guo, *Catal. Lett.*, 1992, **12**, 297.
16 J. Soria, J. M. Coronado and J. C. Conesa, *J. Chem. Soc., Faraday Trans.*, 1996, **92**, 1619.
17 K. H. Jacob, E. Knözinger and S. Benfer, *J. Chem. Soc., Faraday Trans.*, 1994, **90**, 2969.
18 J. Kondo, H. Abe, Y. Sakata, K. Maruya, K. Domen and T. Onishi, *J. Chem. Soc., Faraday Trans.*, 1988, **84**, 511.
19 V. Bolis, C. Morterra, M. Volante, L. Orio and B. Fubini, *Langmuir*, 1990, **6**, 695.
20 D. Spielbauer, G. Mekhemer, M. Zaki and H. Knözinger, *Catal. Lett.*, 1996, **40**, 71.
21 C. Morterra, L. Orio and C. Emanuel, *J. Chem. Soc., Faraday Trans.*, 1990, **86**, 3003.
22 V. Kamble, N. Gupta, V. Kartha and R. Iyer, *J. Chem. Soc., Faraday Trans.*, 1993, **89**, 1143.
23 A. Badri, C. Binet and J. C. Lavalley, *J. Phys. Chem.*, 1996, **100**, 8363.

Paper 7/08208H; *Received* 14*th November*, 1997